

# Simultaneous analytical characterisation of two ultrashort laser pulses using spectrally resolved interferometric correlations

Ivan Amat-Roldan, David Artigas, Iain G. Cormack, and Pablo Loza-Alvarez.

ICFO-Institut de Ciències Fotòniques, and Department of Signal Theory and Communications, Universitat Politècnica de Catalunya. 08860 Castelldefels (Barcelona) Spain

**Abstract:** In this paper we discuss in detail the underlying theory of a novel method that allows the characterizing of ultrashort laser pulses to be achieved in an analytical way. MEFISTO, (measuring the electric field by interferometric spectral trace observation) is based on a Fourier analysis of the information contained in a spectrally resolved interferometric correlation and can be applied to both situations: the characterization of an unknown pulse (MEFISTO) or to the simultaneous characterization of two different unknowns pulses (Blind-MEFISTO). The theoretical development and experimental practical implications are discussed in both situations.

© 2006 Optical Society of America

**OCIS codes:** (100.5070) Phase retrieval; (190.1900) Diagnostic applications of nonlinear optics; (320.7100) Ultrafast measurements.

---

## References and links

1. J.-C. Diels, E. W. Van Stryland, and D. Gold, "Investigation of the parameters affecting subpicosecond pulse duration of passively mode-locked dye laser," in *Proceedings, First International Conference on Picosecond Phenomena*, (Springer-Verlag, New York, 1978), pp. 117–120.
2. J.-C. Diels, E. W. Van Stryland, and G. Benedict, "Generation and measurement of 200 femtosecond optical pulses," *Opt. Commun.* **25**, 93-95 (1978).
3. C. Iaconis, V. Wong, and I. A. Walmsley, "Direct interferometric techniques for characterizing ultrashort optical pulses," *IEEE J. Sel. Top. Quantum Electron.* **4**, 285-294 (1998).
4. C. Iaconis and I. A. Walmsley, "Spectral phase interferometry for direct electric-field reconstruction of ultrashort optical pulses," *Opt. Lett.* **23**, 792–794 (1998).
5. D. J. Kane and R. Trebino, "Single-shot measurement of the intensity and phase of an arbitrary ultrashort pulse by using frequency-resolved optical gating," *Opt. Lett.* **18**, 823–825 (1993).
6. J. L. A. Chilla and O. E. Martinez, "Direct determination of the amplitude and the phase of femtosecond light pulses," *Opt. Lett.* **16**, 39–41 (1991).
7. G. Stibenz, G. Steinmeyer, "Interferometric frequency-resolved optical gating," *Opt. Express* **13**, 2617-2626 (2005).
8. I. Amat-Roldán, I. G. Cormack, P. Loza-Alvarez, E. J. Gualda, and D. Artigas, "Ultrashort pulse characterisation with SHG collinear-FROG," *Opt. Express* **12**, 1169–1178 (2004).
9. I. Amat-Roldán, I. G. Cormack, P. Loza-Alvarez, and D. Artigas, "Starch-based second-harmonic-generated collinear frequency-resolved optical gating pulse characterization at the focal plane of a high-numerical-aperture lens," *Opt. Lett.* **29**, 2282–2284 (2004).
10. I. Amat-Roldán, I. G. Cormack, P. Loza-Alvarez, and D. Artigas, "Measurement of electric field by interferometric spectral trace observation," *Opt. Lett.* **30**, 1063-1065 (2005).
11. D. T. Reid, P. Loza-Alvarez, C. T. A. Brown, T. Beddard, and W. Sibbett, "Amplitude and phase measurement of mid-infrared femtosecond pulses by using cross-correlation frequency-resolved optical gating," *Opt. Lett.* **25**, 1478–1480 (2000).
12. K. W. DeLong, R. Trebino and W. E. White, "Simultaneous recovery of two ultrashort laser pulses from a single spectrogram," *J. Opt. Soc. Am. B* **12**, 2463–2466 (1995).
13. A. V. Oppenheim and R. W. Schaffer, *Digital Signal Processing* (Prentice-Hall, 1975).
14. B. Seifert, H. Stolz, M. Tasche, "Nontrivial ambiguities for blind frequency-resolved optical gating and the problem of uniqueness," *J. Opt. Soc. Am. B* **21**, 1089-1097 (2004).

## 1. Introduction

Interferometric techniques have always been used to characterize ultrashort laser pulses [1-2]. For a long time it was thought that only pure interferometric characterization techniques such as SPIDER [3-4] were able to directly retrieve the phase and amplitude information from an ultrashort laser pulse. Other characterization techniques, specifically time-frequency measurements such as FROG, have required iterative retrieval algorithms to extract phase information [5, 6]. Recently, there has been significant interest in analyzing information within a frequency resolved interferometric autocorrelation traces and has resulted in a new iterative retrieval algorithm being developed [7] as well as a methodology to convert such a trace into a standard FROG trace [8-9]. Additionally, we have recently experimentally demonstrated a new interferometric-based pulse characterisation technique called MEFISTO (Measuring the electric field by interferometric spectral trace observation) [10]. MEFISTO has allowed for the first time, the analytical characterization of an unknown ultrashort pulse from a time-frequency representation of a pulse.

MEFISTO, as SPIDER, allows the pulse information to be directly extracted from experimental data. However, unlike SPIDER, it is based on recording a time-frequency measurement of the pulse which makes it strongly related to FROG. This ambivalent nature makes it possible to share some of the advantages attributed to both methodologies. On one side, as in SPIDER, the extraction of the phase can be directly performed without the need of an iterative retrieval algorithm. On the other side, MEFISTO possesses the same error checking capabilities and simple experimental arrangement as FROG allowing it to be used in a broader range of applications where collinear geometry is required [9]. Furthermore, as we show in this paper, the time-frequency nature of the method makes possible, as in XFROG [11, 12], the simultaneous characterization of two unknown ultrashort pulses, a technique we refer to as blind-MEFISTO.

The aim of this paper is to outline the theoretical background and discuss the retrieving analytical procedure and practical implications in detail. Our main goal here is to present the generalized theory for Blind-MEFISTO and then go on to discuss the particular properties of the degenerate case where the two pulses are equal (MEFISTO). For this purpose, the paper has been organized as follows: In section 2, we develop the general theory. This is followed by an example of the blind-MEFISTO retrieval. In section 4 some experimental and practical considerations are pointed out. A discussion on the degenerate case is presented in section 5. Finally, general conclusions are given.

## 2. Theory

MEFISTO is based on the Fourier analysis of a spectrally resolved interferometric correlation trace. The experimental set up to obtain such a trace can be seen in Fig. 1.

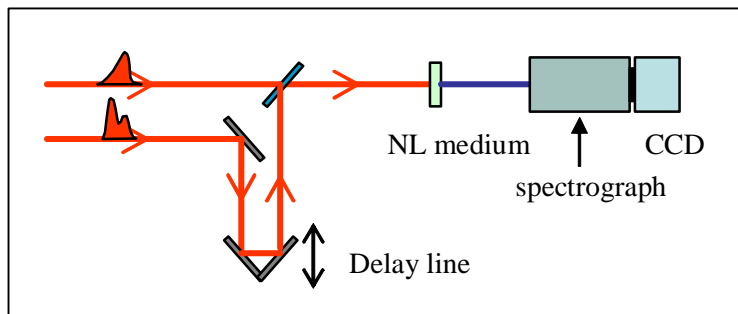


Fig. 1. Typical experimental set up needed to obtain a Frequency resolved interferometric correlation trace.

Two pulses interact collinearly within a nonlinear medium, one of them after passing through a delay arm. The second harmonic generated signal is then directed to a spectrograph

to obtain the interferometric time-frequency trace in terms of the time-delay  $\tau$  and the frequency  $f$ . An example of the resulting trace can be seen in Fig. 2(a). In a general case, this trace can be mathematically described as

$$I^{SHG}(f, \tau) = \chi \cdot \left| F_t \left\{ \left[ E(t) \exp[i2\pi f_1 t] + G(t - \tau) \exp[i2\pi f_2 (t - \tau)] \right]^2 \right\} \right|^2 \quad (1)$$

where  $E(t)$  and  $G(t)$  are the slowly varying amplitude of the complex electric field centered at the frequencies  $f_1$  and  $f_2$ . The Fourier transform with respect to the variable  $t$  is indicated by  $F_t$  and  $\chi$  is related with the conversion efficiency in the nonlinear process. Note that the two interfering pulses  $E(t)$  and  $G(t)$  can be either different, what is referred to us as Blind-MEFISTO, or equal, which is the degenerate case that for simplicity is solely named MEFISTO. In Blind-MEFISTO, phase matching must be achieved for all the cross-terms in (1) and, as we will show, the new information carried on the interferometric terms will allow the simultaneous analytical determination of  $E(t)$  and  $G(t)$ . In general, this should restricts the use of Blind-MEFISTO to the case in which the central frequencies of  $E(t)$  and  $G(t)$  are equal ( $f_1 = f_2 = f_0$ ).

We start our analysis by calculating the Fourier transform of Eq. (1) in the  $\tau$  axis, i.e.,  $Y^{SHG}(f, \kappa) = F_\tau \{ I^{SHG}(f, \tau) \}$ . The resulting expression consist of 5 main spectral components [see Fig. 2(b)] at delay-frequencies  $\kappa = 0, \pm f_0$  and  $\pm 2f_0$ . Since the interferometric trace [Fig. 2(a)] is real, the negative spectral components in Fig. 2(b) are the complex conjugate of the positive ones. We therefore only need to focus upon one of the components (either the positive or the negative) to analyze the information enclosed in the transformed trace. Each of these terms contain information of the pulse phase and intensity and their use will depend on the particular experimental conditions. To highlight the information enclosed in  $Y^{SHG}(f, \kappa)$ , we will separately focus on the mathematical expression for each component and analyze their possibilities.

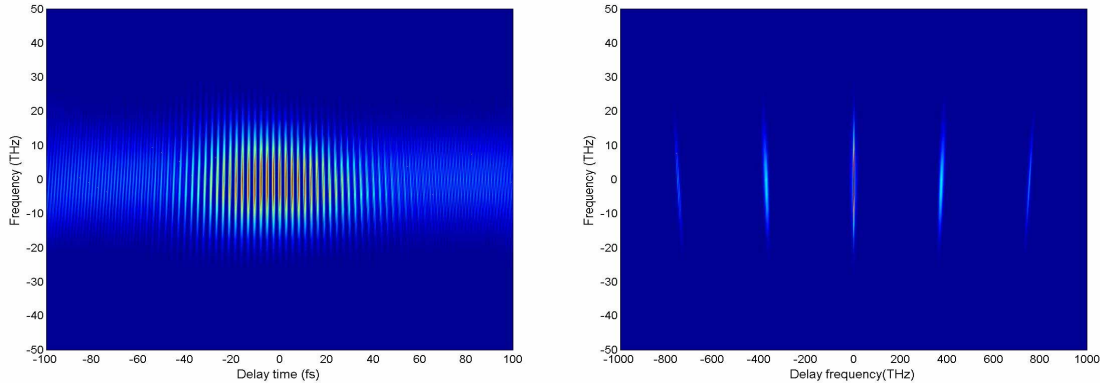


Fig. 2. (a) Frequency resolved interferometric correlation trace and (b) its Fourier transform in the delay-frequency axis, showing the different spectral components.

We start analyzing the component at  $\kappa = 0$ , which can be written as:

$$Y_{DC}^{SHG}(f, \kappa) = \chi \cdot \left( |E_{SHG}(f)|^2 + |G_{SHG}(f)|^2 \right) \delta(\kappa) + 4\chi \int_{-\infty}^{\infty} df' E(f') G(f-f') E^*(f'-\kappa) G^*(f-f'+\kappa) \quad (2)$$

where the second harmonic of the two unknown fields  $E_{SHG}(f)$  and  $G_{SHG}(f)$ , are related with the fundamental pulse following  $F_{SHG}(f) = \int_{-\infty}^{\infty} df' F(f') F(f-f')$ , with  $f$  corresponding to the base-band frequency [13]. The second term in Eq. (2) includes the standard XFROG trace that has been used to characterize ultra short laser pulses [11,12]. It is worth noting that this term, with the use of adequate phase matching conditions, can be obtained even in the case where the spectra of the two pulses do not overlap ( $f_1 \neq f_2$ ) allowing XFROG to be used to characterise pulses that have differing central frequencies. In a previous paper we outlined a filtering procedure capable to extract the FROG term from the  $\kappa = 0$  component in the degenerate case ( $E(t) = G(t)$ ). This technique named as CFROG [8] can straightforwardly be extended to obtain the XFROG term. However, when retrieving the pulses, it again relies upon the use of retrieval algorithms since the integral on Eq. (2) does not allow the analytical determination of  $E(t)$ .

We continue our analysis by focusing upon the spectral component of  $Y^{SHG}(f, \kappa)$  at  $\kappa \approx 2f_0$ . This component can be written as

$$Y_{\kappa \approx 2f_0}^{SHG}(f, \kappa) = \chi \cdot E_{SHG}(f) G_{SHG}^*(f) \delta(f - \kappa + 2f_0) \quad (3)$$

This expression corresponds to a straight line in the transformed trace [Fig. 2(b)] given by  $\kappa = f + 2f_0$ . This term can be used for different purposes. Firstly, in an experimental trace, the divergence from an ideal delta function gives a measure of the pulse jitter, as suggested in Ref. [7], or in general, the quality of the measurement. In addition, any deviation from a linear dependency between  $\kappa$  (real frequency) and  $f$  (base band frequency) will indicate a spectrograph miss-calibration. This component can also determine  $E(t)$  when the gating function,  $G(t)$ , is already known. It can therefore be used as a further verification of the blind-MEFISTO retrieval by checking that the two pulses fulfill

$$E(t) = \sqrt{F_f^{-1} \left\{ \frac{Y^{SHG}(f, \kappa = f + 2f_0)}{\chi \cdot F_t \{ (G(t))^2 \}} \right\}} \quad (4)$$

Although the terms at  $\kappa = 0$  and  $\pm 2f_0$  are useful to obtain some pulse information, it is the component at  $\kappa \approx f_0$  of  $Y^{SHG}(f, \kappa)$  that allows the simultaneous analytical characterization of two unknown ultrashort pulses. The mathematical expression for this component can be written as:

$$Y_{\kappa \approx f_0}^{SHG}(f, \kappa) = 2\chi \cdot E_{SHG}(f) E^*(f + f_0 - \kappa) G^*(\kappa - f_0) + 2\chi \cdot G_{SHG}^*(f) G(f + f_0 - \kappa) E(\kappa - f_0) \quad (5)$$

This equation shows the main advantage of Fourier transforming the trace as was done in Fig. 2(b): All the convolutions that appear in the time domain have been transformed into products in the frequency domain. This isolates the individual pulse fields and makes it possible to resolve analytically. To show this, we firstly write all the involved complex magnitudes in polar form, i.e.,  $E(f) = E_0 U(f) \exp(i\phi(f))$ ,  $G(f) = G_0 V(f) \exp(i\gamma(f))$ , and

equivalently for the harmonic pulses  $E_{SHG}(f) = E_0^{SHG} U_{SHG}(f) \exp(i\phi_{SHG}(f))$  and  $G_{SHG}(f) = G_0^{SHG} V_{SHG}(f) \exp(i\gamma_{SHG}(f))$ . Here, for convenience, all spectral profiles  $U(f)$  are normalized at the central base-band frequency ( $U(f=0) = 1$ ). Then, taking  $Y^{SHG}(f, \kappa) = R(f, \kappa) \exp(i\theta(f, \kappa))$ , Eq. (5) can be written as

$$\begin{aligned} R(f, \kappa) = & 2\chi_1 U_{SHG}(f) U(f + f_0 - \kappa) V(\kappa - f_0) \times \\ & \exp[\phi_{SHG}(f) - \phi(f + f_0 - \kappa) - \gamma(\kappa - f_0) - \theta(f, \kappa)] + \\ & 2\chi_2 \cdot V_{SHG}(f) V(f + f_0 - \kappa) U(\kappa - f_0) \times \\ & \exp[-\gamma_{SHG}(f) + \gamma(f + f_0 - \kappa) + \phi(\kappa - f_0) - \theta(f, \kappa)] \end{aligned} \quad (6)$$

Here we have defined two parameters  $\chi_1 = \chi E_0^{SHG} E_0 G_0$  and  $\chi_2 = \chi G_0^{SHG} E_0 G_0$ , which can be understood as effective conversion efficiency parameters. In section 4, we will go on to describe a procedure to obtain  $\chi_1$  and  $\chi_2$  from the experimental trace. In what follows, and for clarity purposes, we will assume that these parameters are known. Under typical lab conditions the normalized spectra profiles,  $U(f)$ ,  $V(f)$ ,  $U_{SHG}(f)$  and  $V_{SHG}(f)$  can be easily measured. As  $R(f, \kappa)$  and  $\theta(f, \kappa)$  are obtained from the interferometric trace, therefore, the only unknowns in Eq. (6) corresponds to the phase of the fundamental and second harmonic pulse, i.e.,  $\phi(f)$ ,  $\gamma(f)$ ,  $\phi_{SHG}(f)$  and  $\gamma_{SHG}(f)$ . In order to fully characterize the pulses these unknowns must be calculated. This can be achieved by first taking two different slices in the transformed space of the interferometric trace, e.g., at  $\kappa = f_0$  and  $\kappa = f_0 - \Delta f$ . Then, by taking the real and imaginary parts in Eq. (6), we can isolate the phase component at  $\kappa = f_0$ , obtaining

$$\phi_{SHG}(f) - \phi(f) - \gamma(0) = \pm \cos^{-1}[\Omega_1(f, \kappa = f_0)] + \theta(f, \kappa = f_0) \quad 7(a)$$

$$\gamma_{SHG}(f) - \gamma(f) - \phi(0) = \pm \cos^{-1}[\Omega_2(f, \kappa = f_0)] - \theta(f, \kappa = f_0) \quad 7(b)$$

and at  $\kappa = f_0 - \Delta f$

$$\phi_{SHG}(f) - \phi(f + \Delta f) - \gamma(-\Delta f) = \pm \cos^{-1}[\Omega_1(f, \kappa = f_0 - \Delta f)] + \theta(f, \kappa = f_0 - \Delta f) \quad 7(c)$$

$$\gamma_{SHG}(f) - \gamma(f + \Delta f) - \phi(-\Delta f) = \pm \cos^{-1}[\Omega_2(f, \kappa = f_0 - \Delta f)] - \theta(f, \kappa = f_0 - \Delta f) \quad 7(d)$$

where we have defined two functions that relate the different pulse spectra and the trace as

$$\Omega_1(f, \kappa) = \frac{R^2(f, \kappa) + 4[\chi_1^2 U_{SHG}^2(f) U^2(f + f_0 - \kappa) V^2(\kappa - f_0) - \chi_2^2 V_{SHG}^2(f) V^2(f + f_0 - \kappa) U^2(\kappa - f_0)]}{4\chi_1 R(f, \kappa) U_{SHG}(f) U(f + f_0 - \kappa) V(\kappa - f_0)}$$

and

$$\Omega_2(f, \kappa) = \frac{R^2(f, \kappa) - 4[\chi_1^2 U_{SHG}^2(f) U^2(f + f_0 - \kappa) V^2(\kappa - f_0) - \chi_2^2 V_{SHG}^2(f) V^2(f + f_0 - \kappa) U^2(\kappa - f_0)]}{4\chi_2 R(f, \kappa) V_{SHG}(f) V(f + f_0 - \kappa) U(\kappa - f_0)}$$

Then, by subtracting Eqs. 7(a) and 7(c) we get

$$\Delta\phi_{\kappa}(f) = \phi(f + \Delta f) - \phi(f) = \pm \cos^{-1}[\Omega_1(f, \kappa = f_0)] \mp \cos^{-1}[\Omega_1(f, \kappa = f_0 - \Delta f)] + \theta(f, \kappa = f_0) - \theta(f, \kappa = f_0 - \Delta f) + \gamma(0) - \gamma(-\Delta f) \quad (8)$$

From this equation the phase for the spectral component  $E(f)$ , i.e.,  $\phi(f)$  can be determined by taking an arbitrary origin  $\phi(0)$  and adding up  $\Delta\phi_{\kappa}(f)$  as

$$\phi(f) = \phi(0) + \sum_{f'=\Delta f}^f \Delta\phi_{\kappa}(f'). \quad (9)$$

In a similar way, by subtracting Eqs. 7(b) and 7(d), we obtain the equation necessary to determine the phase increment for  $G(f)$  in terms of the frequency as

$$\Delta\gamma_{\kappa}(f) = \gamma(f + \Delta f) - \gamma(f) = \pm \cos^{-1}[\Omega_2(f, \kappa = f_0)] \mp \cos^{-1}[\Omega_2(f, \kappa = f_0 - \Delta f)] - \theta(f, \kappa = f_0) + \theta(f, \kappa = f_0 - \Delta f) + \phi(0) - \phi(-\Delta f) \quad (10)$$

and, as in the previous case, by taking an arbitrary origin  $\gamma(0)$  find the spectral phase components as

$$\gamma(f) = \gamma(0) + \sum_{f'=\Delta f}^f \Delta\gamma_{\kappa}(f'). \quad (11)$$

Notice that the terms  $\gamma(0) - \gamma(-\Delta f)$  and  $\phi(0) - \phi(-\Delta f)$  in eqs. (8) and (10) are unknown constants. These terms add a linear spectral phase shift that only affects the electric field time origin and therefore they can be decided arbitrarily without affecting the shape of the temporal pulse envelope. Equations (8-11) are the principal result of this work showing that to simultaneously characterize two different pulses in an analytical way is possible.

### 3. Simultaneous characterization of two unknown pulses: blind-MEFISTO

In this section we will numerically go through an analytical retrieval step by step in order to show details of how the method should be performed in an experimental case.

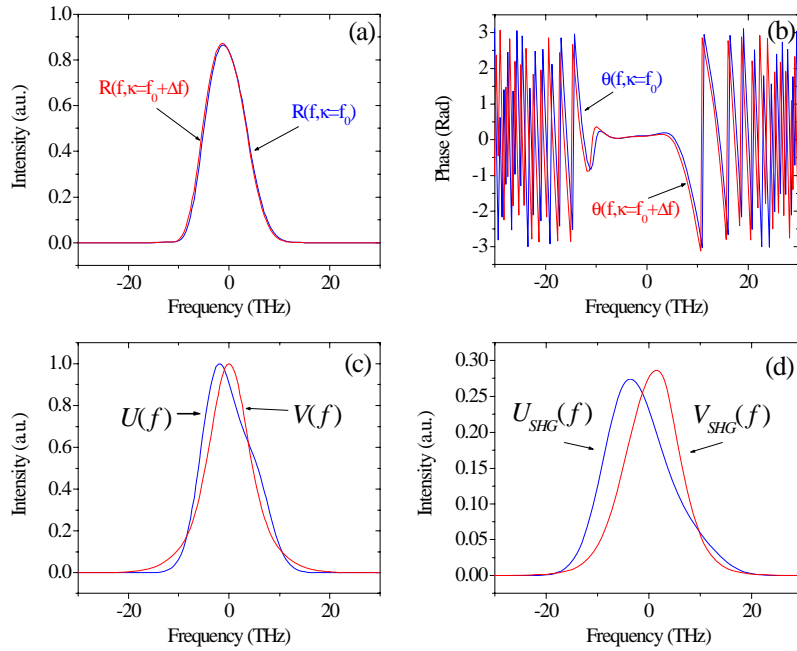


Fig. 3. Experimental data necessary to solve Eqs. (8) and (10). In (a) we show the amplitude and in (b) the phase corresponding to the two slices at  $\kappa = f_0$  and  $\kappa = f_0 + \Delta f$  obtained from the transformed trace in Fig. 2(b). We also show the spectra for the two fundamental pulses (c) and at the SHG frequency (d).

First, as commented we need to take the two slices (at  $\kappa = f_0$  and at  $\kappa = f_0 + \Delta f$ ) of the Fourier transformed interferometric trace shown in Fig. 2(b). The amplitude of the trace  $R(f, \kappa)$  and the phases  $\theta(f, \kappa)$  are respectively shown in Fig. 3 (a) and 3(b) at  $\kappa = f_0$  and  $\kappa = f_0 - \Delta f$ . In addition, to evaluate the  $\Omega_1(f, \kappa)$  and  $\Omega_2(f, \kappa)$  functions, the two fundamental pulses spectra are needed [Fig. 3(c)], which must be obtained experimentally. The two spectra of the second harmonic pulses [Fig. 3(d)] and the parameters  $\chi_1$  and  $\chi_2$  can be either obtained experimentally or directly from the interferometric trace using the method outlined in section 4 (Eqs. 15-16).

In an experimental case  $\Omega_1(f, \kappa)$  and  $\Omega_2(f, \kappa)$  are therefore evaluated using solely experimental data. The resulting  $\Omega_1(f, \kappa)$  and  $\Omega_2(f, \kappa)$  function are shown, respectively, in Figures 4(a) and 4(b), at  $\kappa = f_0$  and  $\kappa = f_0 - \Delta f$ .

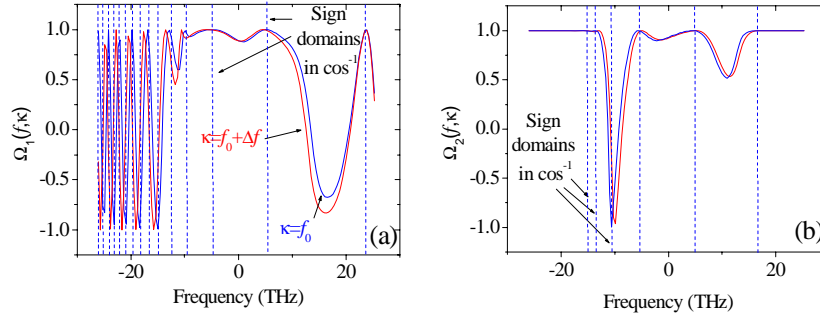


Fig. 4. (a) Function  $\Omega_1(f, \kappa)$  and (b)  $\Omega_2(f, \kappa)$  at  $\kappa = f_0$  and  $\kappa = f_0 + \Delta f$ . Dashed lines shows the division between domains where the function  $\cos^{-1}[\Omega(f, \kappa = f_0)]$  alternates the sign.

Note that the results shown in Figs. 3(b), 4(a), and 4(b) are the necessary data to compute the phase increments in Eqs. (8) and (10). Then, these increments are used in Eqs. (9) and (11), to built up the spectral phases for both pulse. Figures 5(a)-5(b) show the calculated spectral phase obtained with our procedure.

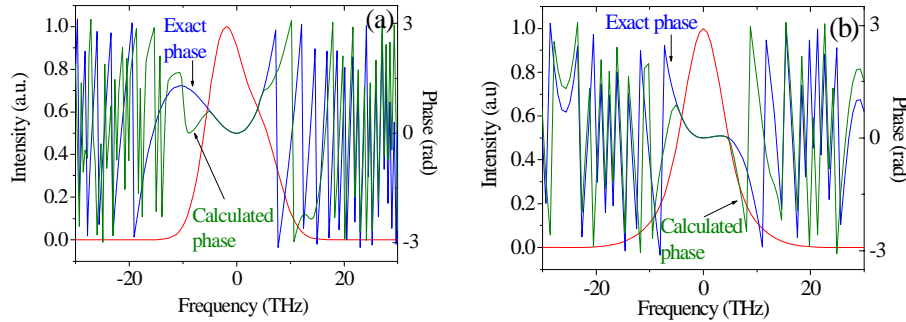


Fig. 5. Retrieved pulses (a)  $E(f)$  and (b)  $G(f)$  using Eqs. (8) and (10) without alternate sign in when changing between the domains shown in Fig. 4.

As can be seen, the results only match with the exact phase within a certain region. This originates from not being able to determine the sign of the phase, which is caused by the sign indetermination related with the  $\cos^{-1}(\Omega)$  function present in Eqs. (8) and (10). Taking into account that  $\cos^{-1}(\Omega)$  should change continuous along the frequency axis in the  $[-\pi, \pi]$  range, the problem can be overcome identifying those points where  $\Omega(f, \kappa)$  get close to 1 or -1 and there is an abrupt change in the slope. In these positions an alternate sign in the  $\cos^{-1}(\Omega)$  function should be performed. These sign-switching points (SSP) define the different domains where the sign in the  $\cos^{-1}(\Omega)$  function changes. These are highlighted in Figures 4(a) and 4(b) with dashed vertical lines. It is worth to mention that finding the right SSP is fundamental to ensure a proper result. In most of the cases, these can be determined by eye inspection or using a simple algorithm. However, for abrupt changes in the  $\Omega(f, \kappa)$  function, this determination can be difficult. This can be the case for pulses with spike spectra or large noise. These two situations are commented in the next section.



After applying the criterion described above to Eqs. (8) and (10), and again using Eqs. (9) and (11) to build up the phase, two possible solutions are available. These two solutions originate from the ambiguity in the sign of Eqs. (8) and (10) at the first domain. However, only one of these solutions is correct. The correct one, observed in Figures 6(a)-6(b), results in the spectral phase that best reproduces the original phase. The second solution, when the other sign is chosen at the first domain, greatly differs from the original phase [Figs. 6(c)-6(d)]. This second solution is a spurious solution of our equation system that correctly reproduces the component at term  $\kappa \approx f_0$  in Fig. 2(b) but it is not solution of the complete interferometric trace. In particular, the pulses in Figs. 6(c)-6(d) do not fulfil Eq. (4), that, as commented before, can be used as error-checking procedure. Experimentally, any source of errors, including the spurious solution, can be detected by numerically generating the interferometric trace using the retrieved pulses and comparing the result with the experimental trace. Equivalently, we can compare the interferometric correlations of the two solutions with the experimental one, which can be directly obtained from the interferometric trace time marginal. We have demonstrated this in Fig. 7. Here, only the interferometric correlation corresponding to the solution in Figs. 6(a)-6(b) is identical to the trace time marginal obtained by integrating the frequency axis of the interferometric trace in Fig. 2(a). Apart from the spurious solution, which can be rejected using the two checking procedures described above, we have not been able to detect other ambiguities as the ones present in XFROG and discussed in Ref. [14].

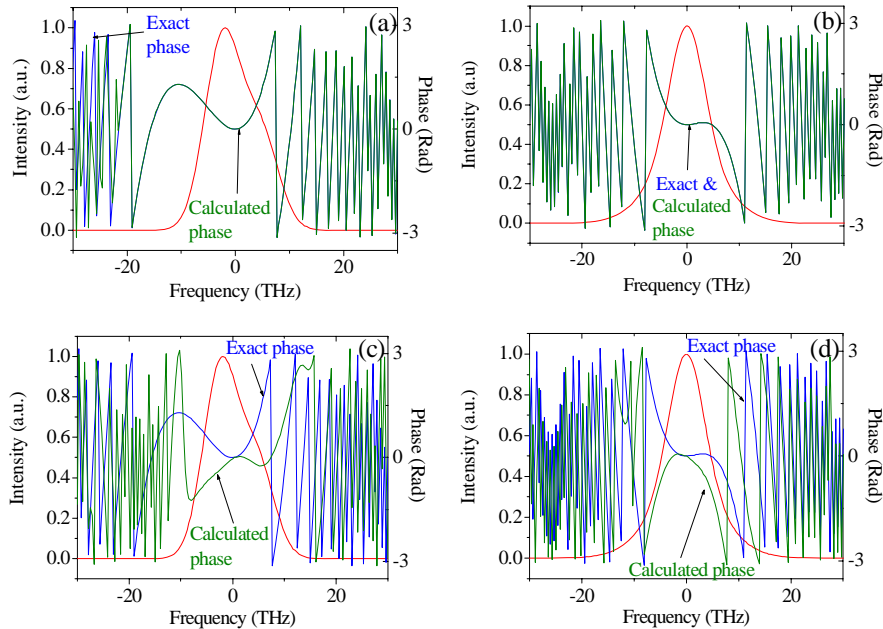


Fig. 6. Obtained pulses alternating the sign at the domains shown in Fig. 4. Result (a)  $E(f)$  and (b)  $G(f)$  using the sign combination (+,-) in Eqs. (8) and (10). The spurious solution is shown in (c)  $E(f)$  and (d)  $G(f)$  using the (-,+) sign combination. Here the discontinuity in the phase corresponds to a  $2\pi$  change.

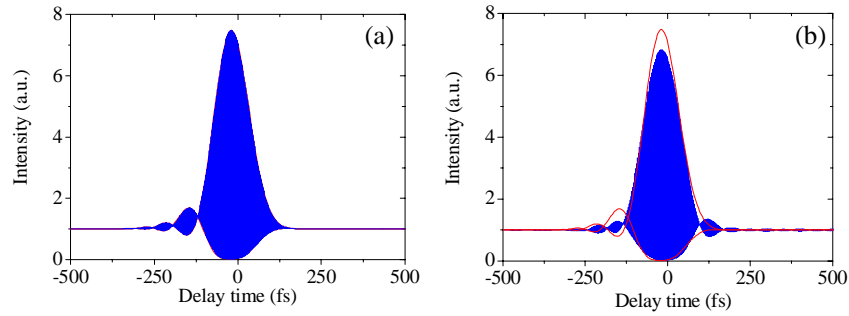


Fig. 7.  $E(f)$  and  $G(f)$  calculated interferometric correlations (blue) and envelope of the interferometric correlation obtained from Fig. 2(a) as the time marginal of the interferometric trace (red). (a) Result using the solution in Figs. 6(a)-6(b). Here the red line coincides with the blue contour and is barely visible. (b) Result using the solution in Figs. 6(c)-6(d).

#### 4. Experimental and practical considerations

In this section we discuss important characteristics of MEFISTO that should be considered to ensure easier and successful pulse retrievals.

##### 4.1. Pulse bandwidth

An important issue to consider is the maximum pulse bandwidth that MEFISTO can successfully characterize. This fundamental limit derives from the necessity to prevent overlap between the different  $\kappa$  components of the transformed trace [see Fig. 2(b)]. Specifically, the two slices at  $\kappa = f_0$  and  $\kappa = f_0 - \Delta f$  must not be affected by the tails of the  $\kappa = 0$  component. In principle, this suggests that the available bandwidth could be equal to the optical carrier, i.e.,  $\Delta\lambda_{\max} \approx \lambda_0$ . However, in practice, this can be affected by the particular spectral shape.

##### 4.2. Frequency resolution

In our analysis we have implicitly considered that the sampling step in the  $f$  and  $\kappa$  axis coincides ( $\Delta\kappa = \Delta f$ ). Initially, the frequency resolution is in fact given by the time-delay span  $\tau_{span}$ , i.e.,  $\Delta\kappa = 1/\tau_{span}$ , which experimentally can differ from the spectrograph resolution. However, by using interpolating techniques to fulfil  $\Delta\kappa = \Delta f$ , the frequency resolution of the method can be extended to  $\Delta f$ .

In the previous section, we pointed out that large changes in the  $\Omega(f, \kappa)$  function can result in errors in determining the SSP. This source of errors can be reduced by increasing the frequency resolution. We must ensure, therefore, that the sampling, and therefore the resolution, results in a reasonable number of points inside the bandwidth.

##### 4.3. Delay resolution.

The delay resolution is determined by the sampling step  $\Delta\tau$ . This is elected following Nyquist criterion to resolve the interferometric fringes:  $\Delta\tau < 1/2f_{\max} < 1/4f_0$ . From the experimental point of view this results in large data sets and acquisition times (of the order of seconds) [10]. The implementation of a faster procedure can be obtained using undersampling techniques in a similar way to the procedure described in Ref. [8]. A detailed investigation of this situation is beyond the scope of this paper and will be reported elsewhere.

#### 4.4. Determining the conversion efficiency parameters $\chi_1$ and $\chi_2$

In our theoretical development, we have considered all the spectral profiles to be normalized to unity at the central wavelength. The energy of each pulse is therefore associated with the spectral amplitudes  $E_0$ ,  $E_0^{SHG}$ ,  $G_0$  and  $G_0^{SHG}$ . These terms, together with the nonlinear coefficient  $\chi$  are included in the conversion efficiency parameters  $\chi_1$  and  $\chi_2$ . Here we will outline how these parameters can be calculated using the  $\kappa = 0$  and  $\kappa = 2f_0$  components of the transformed interferometric trace. To achieve this we must first define three separate equations, two that are derived from the  $\kappa = 0$  term and one that is derived from the  $\kappa = 2f_0 + f$  term. Firstly, using the same procedure outlined in Ref. [8], the two contributions to the  $\kappa = 0$  term in Eq. (2) can be separated. The first part, involving the delta function, when  $\kappa = 0$  gives

$$Y_{\delta}^{SHG}(f, \kappa = 0) = \chi \cdot \left( (E_0^{SHG})^2 U_{SHG}^2(f) + (G_0^{SHG})^2 V_{SHG}^2(f) \right) \quad (12)$$

and the second part, involving the CFROG information, when  $\kappa = 0$  and  $f = 0$ , yields,

$$Y_{CFROG}^{SHG}(0,0) = 4\chi E_0^2 G_0^2 P \quad (13)$$

where  $P = \int_{-\infty}^{\infty} df' U^2(f') V^2(-f')$  can be experimentally determined from the experimental spectra  $I_E(f) = U^2(f)$  and  $I_G(f) = V^2(f)$ . The third equation is obtained by looking at the component at  $\kappa = 2f_0 + f$  and taking its modulus;

$$\left| Y_{\kappa=2f_0}^{SHG}(f, k = 2f_0 + f) \right| = \chi \cdot E_0^{SHG} G_0^{SHG} U_{SHG}(f) V_{SHG}(f) \quad (14)$$

After some algebra, Eq. (12)-Eq. (14) lead to

$$\chi_1^2 U_{SHG}^2(f) = \frac{Y_{CFROG}^{SHG}(0,0)}{8P} \left[ Y_{\delta}^{SHG}(f,0) \pm \sqrt{(Y_{\delta}^{SHG})^2(f,0) - 4(Y_{\kappa=2f_0}^{SHG}(f,2f_0+f))} \right] \quad (15)$$

$$\chi_2^2 V_{SHG}^2(f) = \frac{Y_{CFROG}^{SHG}(0,0)}{8P} \left[ Y_{\delta}^{SHG}(f,0) \mp \sqrt{(Y_{\delta}^{SHG})^2(f,0) - 4(Y_{\kappa=2f_0}^{SHG}(f,2f_0+f))} \right] \quad (16)$$

where all terms on the right hand side are experimental parameters. The sign before the square root depends on the peak intensities of the two second harmonic pulses and must be chosen accordingly so that when, for example,  $I_E^{SHG} > I_G^{SHG}$  then  $\chi_1 > \chi_2$ . By determining Eqs. (15) and (16) we have shown how it is possible to evaluate the functions  $\Omega_1(f, \kappa)$  and  $\Omega_2(f, \kappa)$  without the need of experimentally measuring the intensities of the second harmonic spectra  $U_{SHG}(f)$  and  $V_{SHG}(f)$ .

#### 4.5. Spectral calibration

An experimental measurement, in general, requires two independent measurements: the two fundamental pulse spectra and the interferometric trace. The need for the exact determination of the  $f_0$  and  $2f_0$  places extreme demands and importance on the spectral calibration. These

demands can be relaxed significantly by evaluating the second term of Eq. (2) at  $\kappa = 0$ , and using it to directly relate  $f_0$  and  $2f_0$  with one another:

$$Y_{FROG}^{SHG}(f, 0) = 4E_0^2 G_0^2 \chi_E(f) \otimes I_G(f) \quad (17)$$

By taking a convolution of the two measured fundamental spectra, an accurate spectral registration can be performed that relates the region of the fundamental spectrum with the region of the second harmonic spectrum, where the interferometric trace is obtained. This property allows the MEFISTO technique to be extremely robust against spectrometer miscalibration.

#### 4.6. Noise.

The presence of noise in the experimental measurement can affect the phase extraction as noise increase the difficulty in determining the SSPs. As an example of the limits that noise impose to the technique we have added white Gaussian noise of 20 dB peak signal-to-noise ratio (SNR) to the slide  $R(f, \kappa \equiv f_0)$ , shown in Fig. 3(a). Under these conditions it was still possible to detect the SSPs and we were able to obtain the spectral phase inside the spectrum bandwidth [Fig. 8(a)]. A further rising in the noise level, increased the difficulty in distinguishing the SSPs. To overcome this problem, we reject the high-frequency noise components by filtering the  $\Omega_1(f, \kappa)$  and  $\Omega_2(f, \kappa)$  functions in the  $f$  axis. This procedure allows the phase to be obtained at noise levels as high as 13 dB SNR, as shown in Fig. 8(b).

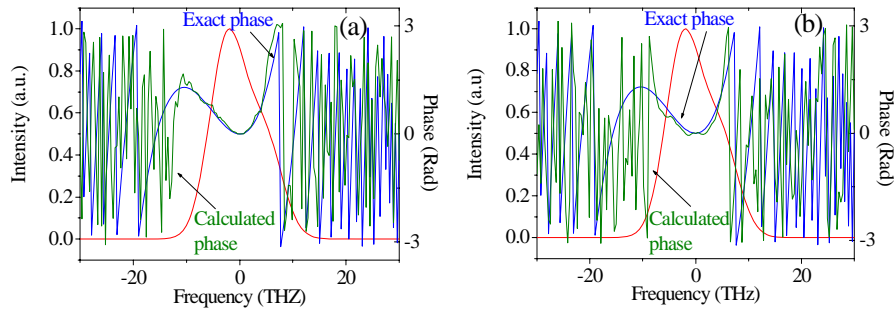


Fig. 8. Retrieved phase for a pulse with (a) 20 dB and (b) 13 dB SNR. Solution in (b) has been obtained by low band pass filtering the functions  $\Omega_1(f, \kappa)$  and  $\Omega_2(f, \kappa)$  in the frequency axis.

### 5. Characterization of an unknown single pulse: degenerate case

This section is devoted to the degenerate case, i.e., when the two interacting pulses are identical. We have experimentally demonstrated MEFISTO for this situation in a previous work [10], here we discuss in more detail some aspect that are particular of this case and are not present in the general case of blind-MEFISTO.

To start, Eqs. (8) and (10) are identical and can be reduced to

$$\Delta\phi_\kappa(f) = \phi(f + \Delta\kappa) - \phi(f) = \pm \cos^{-1}[\Omega(f, \kappa = f_0)] \mp \cos^{-1}[\Omega(f, \kappa = f_0 - \Delta\kappa)] + \phi(0) - \phi(-\Delta\kappa) \quad (18)$$

In the degenerated case we must take into account that the interferometric trace is symmetric with respect to the delay axis  $\tau$  thus its Fourier transform must be real. This has two consequences. First, the upper term in the  $\Omega(f, \kappa)$  functions is directly  $Y^{SHG}(f, \kappa)$ , where  $\Omega(f, \kappa)$  now is written as

$$\Omega(f, \kappa) = \frac{Y^{SHG}(f, k)}{4\chi_{eff} U_{SHG}(f) U(f + f_0 - \kappa) U(\kappa - f_0)}$$

with  $\chi_{eff} = \chi E_0^{SHG} E_0^2$ . In an experimental situation, any imaginary component in  $Y^{SHG}(f, \kappa)$  can be attributed to experimental errors. This is because the interferometric nature of this technique requires having a perfectly centered trace, exact delay steps, no laser instabilities, etc. In this situation, when the center of the delay axis is accurately known, the imaginary part can be omitted. This is the equivalent to the symmetrization process performed in the FROG technique. Retaining the absolute value is however preferred in most of the cases since experimental measurement are never performed under an ideal conditions and the delay origin is unknown. The second consequence of the trace being symmetric is that a positive and negative sign in front of Eq. (18) will give the as result  $E(f)$  and  $E^*(f)$ . This is equivalent to the intrinsic ambiguity that appears in SHG-FROG measurements.

As with blind-MEFISTO, an important factor that affects the determination of  $\Omega(f, \kappa)$  is the effective conversion efficiency parameter  $\chi_{eff}$ . In the degenerate case, the procedure to obtain  $\chi_{eff}$  is very much simplified. In contrast to blind-MEFISTO where an external measurement of the fundamental spectra  $U^2(f)$  is required, the degenerate case allows all the information to be directly obtained from the experimental interferometric trace. This is achieved as follows. First, the amplitude of the second harmonic pulse are obtained from the term at  $\kappa = 2f_0 + f$ , resulting in

$$\sqrt{\chi} \cdot E_0^{SHG} U_{SHG}(f) = \sqrt{Y_{\kappa=2f_0}^{SHG}(f, k = 2f_0 + f)} \quad (19)$$

By normalizing using  $U_{SHG}(f = 0) = 1$ , the spectral profile  $U_{SHG}(f)$  and the factor  $\sqrt{\chi} \cdot E_0^{SHG}$  needed to find  $\chi_{eff}$  are obtained. Second, the term at  $\kappa = 0$  in the degenerate case results in

$$Y_{FROG}^{SHG}(f, \kappa = 0) = 4\chi E_0^4 \int_{-\infty}^{\infty} df' U^2(f') U^2(f - f') = 4\chi E_0^4 \cdot U^2(f) \otimes U^2(f). \quad (20)$$

By using the inverse Fourier transform to deconvolve (20) we obtain:

$$\sqrt{\chi} E_0^2 U^2(f) = \frac{1}{2} F_t \left\{ \sqrt{F_f^{-1} \{ Y_{FROG}^{SHG}(f, 0) \}} \right\} \quad (21)$$

Here again, by normalising  $U(f = 0) = 1$ , the spectral profile of the fundamental pulse  $U(f)$  and the factor  $\sqrt{\chi} \cdot E_0^2$  needed to finally find  $\chi_{eff}$  are obtained. By not requiring an extra spectral measurement, all the data used for the pulse measurement is contained within a single set of data. This helps keep everything self-consistent and as a consequence reduces the risk of erroneous errors entering into the final results.

Finally, as in Blind-MEFISTO, the degenerate case can compare the experimental and numerically generated interferometric traces to check the validity of the method. As commented, the experimental interferometric auto / cross correlation trace is obtained by integrating the trace in frequency. This can be compared with the one numerically obtained from the retrieved pulse. With the degenerate case however an even simpler check can be made by making use of the intrinsic 8:1 ratio that interferometric autocorrelation must have. By integrating the experimental data to obtain the time marginal immediately after acquisition, it is possible to check for the 8:1 ratio. If the ratio is not correct, the data can immediately be discarded and taken again. It should also be noted that in the degenerate case, the use of Eq. (4) as an error checking procedure is not possible, since this component always results in the second harmonic intensity spectrum.

## 5. Conclusions

In this work we have outlined, the theory and procedure of MEFISTO, a method that allows the complex amplitude of two unknown ultrashort pulses with similar central frequency to be simultaneously obtained. Its time-frequency and interferometric ambivalent nature leads to a technique that possesses advantages and properties characteristic of interferometric techniques as SPIDER, as well as time-frequency measurements as FROG. In this sense, similar to interferometric techniques, the method enables the analytical extraction of pulse information without the need of an iterative retrieval algorithm. Similar to time-frequency techniques, it can be applied to simultaneously characterize two unknown pulses (blind MEFISTO) and enjoys extended error-checking capabilities. In addition, MEFISTO is based on a simpler experimental set up as it is based on a collinear arrangement.

The MEFISTO methodology relies on a Fourier analysis after obtaining a spectrally resolved interferometric correlation trace. In particular, we have described the general theory for blind-MEFISTO, pointing out the use of the different terms obtained during the theoretical development. Practical considerations have been discussed. These include spectral calibration, resolution (temporal and spectral), maximum bandwidth, sign indeterminations, possible problems with pulses whose spectra present abrupt changes, error checking procedures, and effect of noise. To manage these experimental limitations, a set of tools have been developed and explained. The analysis has also demonstrated that the method is not affected by some of the non-trivial ambiguities that are present in other techniques [14]. The particular properties of the degenerate case have also been analyzed to highlight additional error-checking capabilities and self-calibrating techniques that help avoid errors entering the pulse measurement.

Finally, we want to stress that this is, to the best of our knowledge, the first analytical methodology capable to simultaneously characterize two unknown ultrashort laser pulses.

## Acknowledgment

This work was supported by the Generalitat of Catalunya, the Spanish Government under grant TIC2003-07485 and by the European Regional Development Fund. P. Loza-Alvarez acknowledges funding from the Spanish Government through the Ramón y Cajal program and I. G. Cormack acknowledges support from the Human Frontier Science Program.